31st Annual International Conference of the IEEE EMBS
Minneapolis, Minnesota, USA, September 2-6, 2009

De-noising of SPECT Images via Optimal Thresholding by Wavelets

H. A.Noubari[1], A. Fayazi[2] and F. Babapour[2]

[1] Department of Electrical Computer Engineering, University of Tehran, and University of British Columbia
[2] Faculty of Engineering, Science and Research Branch, Islamic Azad University, P. O. Box 14515-775, Tehran, Iran

Abstract— **Single photon emission computed tomography (SPECT) imaging provides functional information and precise physiological uptake of radioactivity in a patient's body. Although SPECT imaging is considered to be highly useful in oncology, but the low signal to noise ratio (SNR) caused by photon noise, introduces considerable compromise in image quality and reduction of diagnostic accuracy. It is necessary to apply appropriate noise reduction algorithm to improve the quality of acquired images. In this paper we have used wavelet based denoising in which PSNAR criteria were utilized to arrive at an optimum thresholding of the coefficient at wavelet domain.**

We have used SIMIND software for simulation of SPECT images and generation of images using cylindrical jaszak phantom. The images were acquired using one million counts of 64×64 matrix size. In this research, simulated images were utilized to construct data dependent optimum threshold level of wavelet coefficients We have compared the results of our thresholding scheme with those obtained by some of commonly used standard denoising schemes in which we show the use of commonly used wavelet-based denoising leads to an inferior noise reduction results as compared with our optimally searched and derived thresholding.

Keywords— **SPECT, Wavelet Transform, Denoising, Optimal thresholding**

I. INTRODUCTION

Wavelet transform is characterized by many unique features that have been applied in wide spectrum of application problems including image processing, compression and noise reduction. This transform also provides an elegant framework for subband analysis in which both high and low frequency components of an image can be analyzed separately. Recently, various wavelet-based methods have been proposed for image enhancement and restoration. Often wavelet image restoration methods utilize thresholding approach in which each wavelet coefficient of the image is compared with a given threshold where it is set to zero if the coefficient is smaller than the chosen threshold, otherwise it is retained using hard denoising or reduced in magnitude by threshold level in soft denosing. The intuition behind such an approach follows from the fact that the wavelet transform is efficient at energy compaction, thus small wavelet coefficients are more likely to be due to noise, and large coefficients are generally due to important image features, such as edges. Originally, Donoho and Johnstone proposed the use of a universal thresholding applied uniformly across the entire wavelet decomposition tree [1, 2]. However the use of different thresholds for different subbands and levels of the wavelet tree was found to be more effective for noise reduction [2, 3, and 8]. Some methods of selecting thresholds that are adaptive to different spatial characteristics have recently been proposed and investigated [5-8]. It was found that such adaptivity in the threshold selection tends to improve the wavelet thresholding performance since it accounts for additional local statistics of the image, such as smooth or edge regions.

In this paper, we used SIMIND [9] software for simulation of SPECT images where we prepared images using simulated cylindrical jaszak (Jaszczak) phantom [9, 10]. The images were acquired using one million counts and in 64×64 matrix size. For reference image we acquired an image with high counts (five million). Then, we reconstructed these images using software that was written in MATLAB. This was followed by using one million counts of images (noisy initial image) along with five million counts of the reference image, where they were normalized and utilized for comparison of results. Two criteria, Root mean square error and peak signal to noise ratio (PSNR) were utilized for reconstructed image quality assessment. For de-noising of noisy image, several wavelets from both orthogonal and biorthogonal series were considered. However, we confined our usage to Db2 and Db3 mainly for high order of moment cancellation of these wavelets

Several programs were written in MATLAB for de-noising. These programs were based on use of different wavelets and three approaches for thresholding (Global thresholding, Level dependent thresholding and optimum thresholding). Then, de-noised images were compared with reference image using MSE and PSNR measures.

II. BASIC CONCEPTS

A. Theory

1. 2-D Discrete Wavelet Transform

A 2-D separable discrete wavelet transform is equivalent to two consecutive 1-D transforms implemented on rows followed by a 1-D column transform. Transform coefficients are obtained by projecting the 2-D input image x(u, v) onto a set of 2-D basis functions that are expressed in tensor product form. (1):

$$\begin{aligned}\phi(u,v) &= \phi(u)\phi(v)\\ \psi_1(u,v) &= \psi(u)\phi(v)\\ \psi_2(u,v) &= \phi(u)\psi(v)\\ \psi_3(u,v) &= \psi(u)\psi(v)\end{aligned} \quad (1)$$

The 2-D DWT can be considered as projection of the image *x (u, v) onto* set of scaling function $\phi(u,v)$ and wavelets $\psi_1(u,v)$, $\psi_2(u,v)$ and $\psi_3(u,v)$. The corresponding

transform coefficients $X(N,j,m)$, $X^{(1)}(N,j,m)$, $X^{(2)}(N,j,m)$ and $X^{(3)}(N,j,m)$ belonging to different subbands of the decomposition can be expressed as follows.

$$\begin{aligned} X(N,j,m) &= \iint x(u,v)2^N \phi(2^N u-j)\phi(2^N v-m)\,dudv \Rightarrow LL \\ X^{(1)}(N,j,m) &= \iint x(u,v)2^N \psi(2^N u-j)\phi(2^N v-m)\,dudv \Rightarrow LH \\ X^{(2)}(N,j,m) &= \iint x(u,v)2^N \phi(2^N u-j)\psi(2^N v-m)\,dudv \Rightarrow HL \\ X^{(3)}(N,j,m) &= \iint x(u,v)2^N \psi(2^N u-j)\psi(2^N v-m)\,dudv \Rightarrow HH \end{aligned} \quad (2)$$

$X(N,j,m)$ are the coarse coefficients that constitute the LL subband. The $X^{(1)}(N,j,m)$ coefficients contain the vertical details and correspond to the LH subband. The $X^{(2)}(N,j,m)$ coefficients contain the horizontal details and correspond to the HL subband. The $X^{(3)}(N,j,m)$ coefficients represent the diagonal details in the image and constitute the HH subband. Thus single-level decomposition at scale (N +1) has four subbands of coefficients as shown in Fig 1.

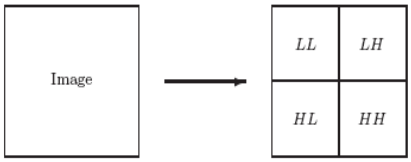

Fig. 1 Single-level 2-D wavelet decomposition (analysis).

The synthesis bank performs the 2-D IDWT to reconstruct $x(u,v) \in V_M$. 2-D IDWT is given in equation (3).

$$\begin{aligned} x(u,v) &= \sum_j \sum_m X(N,j,m)2^N \phi(2^N u-j)\phi(2^N v-m) \\ &+ \sum_{i=N}^{M-1} \sum_j \sum_m \begin{bmatrix} X^{(1)}(i,j,m)2^i \psi(2^i u-j)\phi(2^i v-m) \\ + X^{(2)}(i,j,m)2^i \phi(2^i u-j)\psi(2^i v-m) \\ X^{(3)}(i,j,m)2^i \psi(2^i u-j)\psi(2^i v-m) \end{bmatrix} \end{aligned} \quad (3)$$

2. The Wavelet Thresholding Process

Wavelet thresholding for image denoising attempts to remove the noise present in the image while preserving most of the image characteristics, regardless of its frequency content. It involves the following steps:

1. Acquire the noisy image.
2. Compute a linear forward discrete wavelet transform of the noisy image.
3. Perform a non-linear thresholding operation on the wavelet coefficients of the noisy image.
4. Compute the linear inverse wavelet transform of the threshold wavelet coefficients.

These simple four-step processes are known as wavelet thresholding or shrinkage. The wavelet denoising process can be summarized as follows:

$$\begin{aligned} & x \rightarrow y = x + w \rightarrow Y = DWT(y) \rightarrow \\ & \hat{X} = T(Y,\lambda) \rightarrow \hat{x} = DWT^{-1}(\hat{X}) \end{aligned} \quad (4)$$

In summary, the wavelet denoising problem can be formulated as follows Design a thresholding transformation $T(.,\lambda)$ with threshold λ, such that:

$$MSE = E\left\| x - \hat{x} \right\|^2 \quad (5)$$

Application of, MSE criteria requires assumption of the underlying distribution of noise content for which it is often assumed to be white Gassian noise. To maintain the white noise structure of noise in coefficient domain, it is also required the use of orthogonal transformation .Proper selection of analyzing wavelets is also to made such that sparsity of the coefficient is insured where important features of the original image such as edges are retained in the denoised signal while noise content is removed as much as possible by suitable thresholding. We have used two measures MSE and PSNR to compare the performance of denoising results. It is shown that the use of standard thresholding strategies both under soft and hard denoising does not yield optimal results. This can be described by noting that while noise content of SPECT images contain white Gaussian noise, however noise content of SPECT images consists mainly of non-stationary Poisson noise that are observed in the projection data i.e. sonograms, they are the main contributor for the loss of image quality in the reconstructed SPECT images. We have compared the performance of standard commonly used denoising schemes with an optimally derived thresholding using MSE and PSNR and have shown that considerable improvements can be obtained by deviating from the standard denoising threshold levels. Below two standard thresholding algorithms are briefly described.

III. MATERIALS AND METHODS

There two standard wavelet thresholding methods often applied for denoising referred to as VisuShrink and LevelShrink differ only in the selection of the threshold λ , and the strategy employed in applying the thresholding operator.

A. *VisuShrink*

The VisuShrink technique consists of applying the soft thresholding operator using the universal threshold:

$$\lambda_{univ} = \sqrt{2\ln(M)} \times \sigma_w \quad (6)$$

Where M is image size and σ_w is the standard deviation of difference between Original image and noisy image that defines the standard deviation of noise and equal 4.35. as originally proposed by Donoho and Johnstone [2].

B. *Level Shrink*

The level-dependent thresholding algorithm, called LevelShrink, proposes the use of different thresholds for different levels of the wavelet tree. Since the content of the various subbands varies from one level to the next, the use of level-dependent thresholds seems more reasonable than the use of a uniform threshold.

One particular level-dependent thresholding scheme, called LevelShrink, is to set the threshold at the j^{th} decomposition level of the wavelet tree as follows [8]:

$$\begin{aligned} \lambda_j &= \sqrt{2\ln(M)} \times \sigma_w \times 2^{-(J-j)/2} \\ &= \lambda_{univ} \times 2^{-(j-j)/2}, \end{aligned} \quad (7)$$

Where J is the total number of decomposition levels and j is the scale level on which the wavelet coefficient for thresholding are located.

As illustrated in Table 1, this scheme uses larger threshold values for the finer scales decomposition tree and smaller thresholds for the more coarse scales of the wavelet tree. Note that for the highest level, the universal threshold is used. However, for the lower levels, the threshold is gradually scaled down.

Table 1: The optimal thresholds for the various wavelet decomposition levels used by the Level Shrink thresholding scheme.

	finer ← Wavelet Decomposition Level → coarse					
Level	6	5	4	3	2	1
Threshold	17.7422	12.5456	8.8711	6.2728	4.4355	3.136

C. Peak Signal-to-Noise Ratio

We have used MSE and PSNR as a measure of the quality of reconstructed image where for an original image u of size m×n and denoised, image $\tilde{u}$ they are given by:

$$MSE = \frac{1}{m \times n} \sum_{i=0}^{m-1} \sum_{j=0}^{n-1} \left\| u_{i,j} - \tilde{u}_{i,j} \right\| \quad (8)$$

$$PSNR = 10\log_{10}\left(\frac{\max(u)}{MSE}\right)^2 = 20\log\left(\frac{\max(u)}{RMSE}\right) \quad (9)$$

Where MAX(u) is the maximum pixel value for an 8 bits/pixel gray-scale image

IV. RESULTS

A. *Exploring the Optimality of the Universal Threshold*

In order to explore the "optimality" of VisuShrink and universal thresholding, the quality of the denoised image, as measured by the RMSE and PSNR using different value of threshold level is examined. The noisy image of "SPECT", as described above was used and the threshold was allowed to span a wide range of values including the universal threshold. Fig. 2 illustrates the results obtained using the hard and soft thresholding approaches. We observe that for the given test image, the optimal thresholds corresponding to the hard and soft thresholding algorithms are lower than the universal threshold adopted by VisuShrink, particularly in the case of soft thresholding.

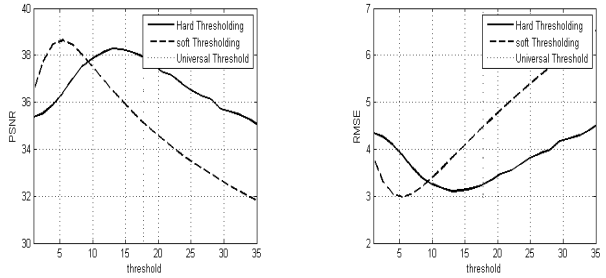

Fig. 2 The dependence of the quality of the denoised image on the selection of the threshold for hard and soft thresholding, using the noisy image of "simulated SPECT".

For the given test image of "SPECT", the optimal thresholds were found to be $\lambda^*_{hard} \approx 12$, for hard thresholding and $\lambda^*_{soft} \approx 6$, for soft thresholding. The ratio between the optimal values o f λ^*_{soft} and λ^*_{hard}, can generally be given by the following s:

$$\lambda^*_{soft} \approx \frac{\lambda^*_{hard}}{2} \quad (10)$$

The above ration between the optimal values of λ^*_{soft} and λ^*_{hard} has also been widely reported in the wavelet thresholding literature [6, 8].

B. *Implementation of different thresholding methods*

Figure 3 illustrates the noisy image and Original image and the profile of noisy image and Original image.

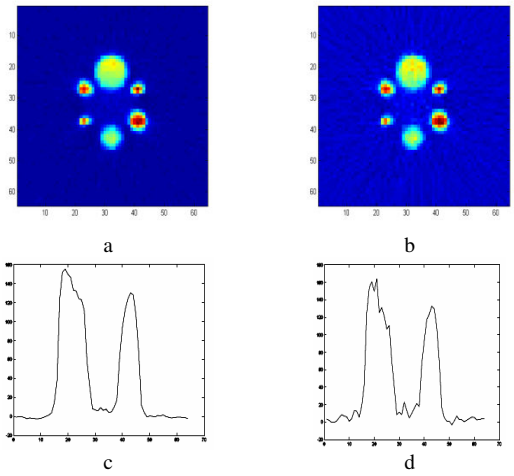

Fig. 3 (a) Original image, (b) noisy image, (c) profile of Original image, (d) profile of noisy image.

Three wavelet thresholding methods (VisuShrink, LevelShrink and optimal thresholding algorithm) were implemented for reconstruction of denoised SPECT image. We note that VisuShrink was found to yield an overly smoothed estimate, especially in case of the soft thresholding.. This is because the universal threshold λ_{univ}, tends to be too high for large values of M, setting to zero many signal coefficients along with the noise. This illustrates a common limitation of VisuShrink widely reported in literature [1, 6, 8].

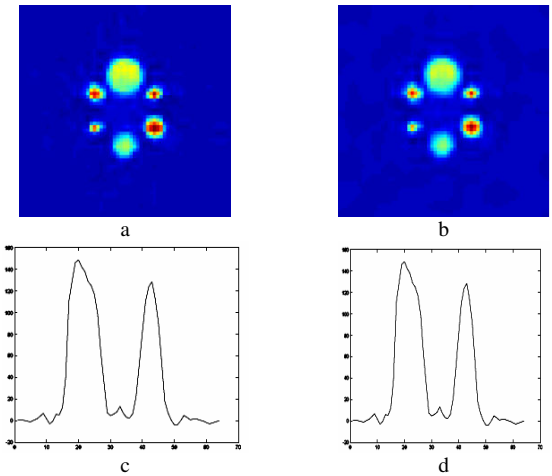

Fig. 4 (a) Visushrink hard thresholding denoised estimates of SPECT, (b) Visushrink soft thresholding denoised estimates of SPECT, (c) Profile of denoised image by Visushrink hard thresholding, (d) Profile of denoised image by Visushrink soft thresholding.

The VisuShrink algorithm was implemented for the purpose of restoring and enhancing the noisy image of "SPECT". Figure 4 illustrates the results corresponding to the hard and soft thresholding methods using the universal threshold ($\lambda_{universal} = 17.7422$).

As described in the previous section, VisuShrink adopts the universal threshold to be used uniformly throughout the wavelet decomposition tree of the noisy image. Intuitively, due to the high variability of the wavelet coefficients across different subbands and decomposition levels, it would be more reasonable, and perhaps more efficient, to use different thresholds for different subbands and levels of the wavelet tree.

Figure 5 illustrates the results obtained by using the hard and soft LevelShrink thresholding the noisy test image of "SPECT".

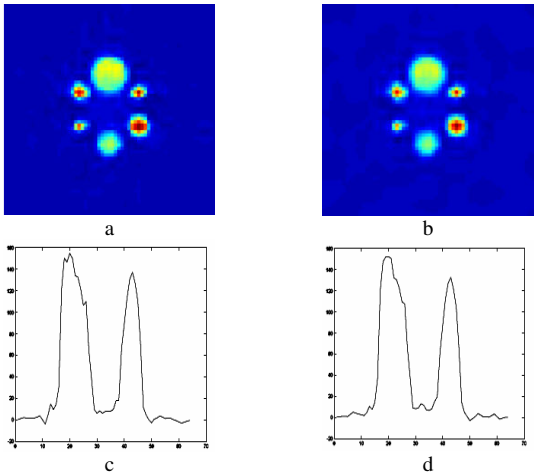

Fig. 5(a) Levelshrink hard thresholding denoised estimates of SPECT, (b) Levelshrink soft thresholding denoised estimates of SPECT, (c) Profile of denoised image by Levelshrink hard thresholding. (d) Profile of denoised image by Levelshrink soft thresholding.

The optimal values of soft and hard thresholds were also used to denoise the test image and the results are illustrated in Figure 6.

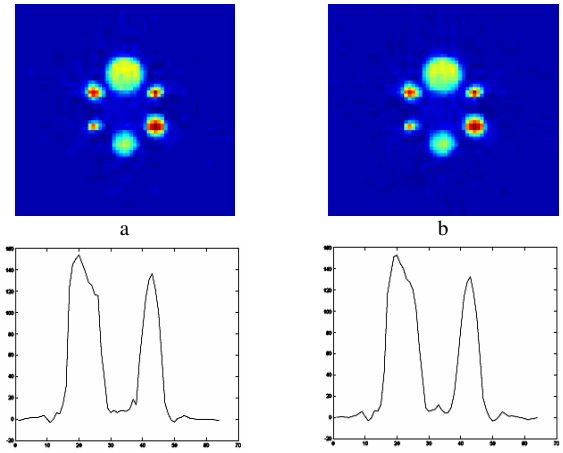

Fig. 6 (a) Optimal Hard threshold denoised estimates of SPECT $\lambda^*_{hard} = 13$. (b) Optimal Soft threshold denoised estimates of SPECT $\lambda^*_{soft} = 5.5$. (c) Profile of denoised image by Optimal hard threshold. (d) Profile of denoised image by soft Optimal threshold.

Table 2 shows the result of Implementation of the various thresholding methods.

Table 2: Comparison between the results obtained by the various wavelet thresholding methods

Thresholding methods	Hard thresholding		Soft thresholding	
	RMSE	PSNR	RMSE	PSSR
Visushrink	3.5251	37.2889	4.4737	35.1147
Levelshrink	3.7104	38.3290	3.9156	36.2748
Optimum thresholding	3.1097	38.6311	2.9775	38.6538

V. CONCLUSIONS

The result of denoising as measured by MSE and PSNR is summarized and compared in table 2. It is seen that the optimally searched threshold levels leads to higher performance in eliminating the noise as compared with both of global thresholding (Visushrink) and level dependent thresholding methods (Leveshrink). In de-noising by optimal thresholding method, the peak signal to noise ratio (PSNR) value for the test image was found to be 38.65 db, as compared with global soft thresholding method (Visushrink) 35.114 db namely an improvement of 9.15 prercentage PSNR and as compared to level dependent thresholding method (Leveshrink) with an improvement of 6.15 percentage in PSNR. Similar improvements are obtained in MSE as given in Table 2. , In summary, it is our conclusion that in practice, it may be necessary to investigate the performance of denoising schemes as to their optimality by changes that may be made around the derived threshold levels. This may lead to improved denoising results and more significantly to an enhanced diagnostics.

REFERENCES

1. D.L. Donoho, “Denoising and soft-thresholding," IEEE Trans. Infor. Theory, vol. 41, pp 613-627, 1995
2. D.L. Donoho, and I.M. Johstone, " Ideal spatial adaptation via wavelet shrinkage," Biometrika, vol. 81, pp 425-455, 1994
3. D.L. Donoho, and I.M. Johstone, " Adapting to unknown smoothness via wavelet shrinkage," Journal of the American Statistical Assoc., vol. 90, no. 432, pp 1200-1224, 1995
4. S.G. Chang, B. Yu, and Martin Vetterli, " Spatially adaptive wavelet thresholding with context modeling for image denoising," IEEE Trans. on Image Proc., vol. 9, no. 9, pp. 1522-1531, 2000.
5. S.G. Chang, B. Yu, and Martin Vetterli, " Adaptive image thresholding for image denoising and compression," IEEE Trans. on Image Proc., vol. 9, no. 9, pp. 1532-1546, 2000.
6. S.G. Chang, B. Yu, and Martin Vetterli, " Bridging compression to wavelet thresholding as a denoising method," in Proc. Conf. Information Sciences Systems, Baltimore, MD, pp. 568-573,1997.
7. S. Zhong, and V. Cherkassky, " Image denoising using wavelet thresholding and model selec tion," Proc. IEEE Int. Conf. on Image Proc. (ICIP), Vancouver, BC, Sept. 2000.
8. S.G. Mallat, A Wavelet Tour of Signal Processing, New York: Academic Press, 1998.
9. www.radfys.lu.se/simind/index.asp.
10. www.biodex.com/radio/phantoms/phantoms_750.htm.